S & M 0587

# Direct Fabrication of Micropatterns and Three-Dimensional Structures Using Nanoreplication-Printing (nRP) Process

Sang Hu Park, Tae Woo Lim, Dong-Yol Yang\*, Shin Wook Yi<sup>1</sup> and Hong Jin Kong<sup>1</sup>

Department of Mechanical Engineering, Korea Advanced Institute of Science & Technology (KAIST), Science Town, Daejon-city 305-701, Korea.

Department of Physics, Korea Advanced Institute of Science & Technology (KAIST), Science Town, Daejon-city 305-701, Korea.

(Received April 10, 2004; accepted November 16, 2004)

*Key words:* nanoreplication printing (nRP), two-photon-absorption polymerization (TPP), three-dimensional microstructure, direct patterning, femtosecond pulse laser

A method for the direct fabrication of submicron-scale detailed patterns without the use of a photomask was developed by means of a nanoreplication-printing (nRP) process. Some patterns can be fabricated easily in the range of several microns inside a polymerizable resin by a scanning process using a volume-pixel (voxel) matrix that is transformed from a bitmap figure file. In the nRP process, liquid monomers are polymerized by the twophoton absorption (TPA) induced using a femtosecond pulse laser. Voxels are merged consecutively by overlapping in a range of several microns to fabricate various patterns, and the resolution of the process can be determined as the diffraction limit of the laser beam used to induce two-photon absorption polymerization (TPP). In this work, a beam expansion technique has been applied to enlarge the working area used to fabricate patterns. The establishment of a mechanism capable of the three-dimensional (3D) fabrication of microstructures by use of a lamination technique, which fabricates a structure layer by layer, has been attempted. The technique does not require the use of sacrificial layers or structures in 3D microstereolithography. Through this work, the usefulness of the nRP process is demonstrated by the fabrication of several patterns and 3D microstructures with a resolution of approximately 200 nm.

<sup>\*</sup>Corresponding author, e-mail address: dyyang@kaist.ac.kr

#### 1. Introduction

Recently, the demand for the fabrication of smaller features relating to nanotechnologies, information technologies, and other precision industries has greatly increased to enable the development of a number of new conceptual and high-value-added products. Photolithography has been recognized as a chief technology for the patterning that is needed to fabricate electronic and optical devices. So far, many devices have been developed utilizing photolithography which has been the major technique of the semiconductor industry since its invention. In addition, many applications of photolithography have been introduced. However, lithography technology is rapidly approaching its fundamental limits with respect to its resolution, the high process cost, and the constraints on arbitrary shaping or patterning for various applications. Although it is difficult to find suitable replacement technologies, there is much demand for new technologies to pattern features on scales less than 100 nm. If cost is not a major concern, there are a few technologies capable of fabricating sub-100 nm features, such as electron-beam lithography and lithography technologies utilizing probe tips.<sup>(1)</sup> For high-throughput, low-cost, and high-resolution lithography, various nanoimprinting technologies have been developed.<sup>(2–5)</sup>

In the past several years, some works have been conducted in nanoscale fabrication technology using two-photon polymerization (TPP) induced with a femtosecond laser. TPP has many advantages as a technique for the direct fabrication of complex three-dimensional (3D) structures on a scale of several microns, which might be difficult to obtain using general miniaturization technologies. There is an increasing demand for techniques which enable the fabrication of submicron structures. Previous works<sup>(6-15)</sup> using TPP have focused on the applications of fabricating complicated 3D structures<sup>(9-11)</sup> and photonic crystals.<sup>(14)</sup> A high-aspect-ratio patterning process has also been conducted using TPP.<sup>(16)</sup> It has recently been reported that a femtosecond laser pulse can be tightly focused onto liquid-state monomers initiating a chemical process by TPP with features close to 100 nm in size. A highly localized area around the center of the focused beam can be solidified by absorbing the threshold energy for polymerization, because the TPP rate is proportional to the square of the laser intensity. Therefore, sub-100-nm resolution can be obtained using a high-numerical-aperture (NA) objective lens without any restraint imposed due to the diffraction limit of the beam.

A nanoreplication-printing (nRP) process utilizing a beam expansion technique was developed in this work for the direct fabrication of nanoprecision patterns on a glass plate without the use of a photomask. A two-tone (black and white) bitmap figure was employed in the nRP process to be transformed as a voxel matrix. In the process, a voxel matrix scanning (VMS) scheme was used to scan along the x-axis and y-axis to generate patterns directly onto a plate. The effectiveness of the nRP process for direct patterning with a resolution of approximately 200 nm was estimated. A laminating technique for the fabrication of a three-dimensional microstructure was attempted to establish a mechanism capable of the fabrication of 3D structures. A 3D honeycomb structure was constructed by stacking laminated layers which were fabricated by the nRP process with a layer thickness of 200 nm. There are a few remaining problems concerning precision in the process of fabricating 3D structures that need to be solved in further studies, such as the shrinkage phenomenon, the surface roughness of the fabricated structure, and beam alignment.

# 2. Theoretical Studies of Nanoreplication-Printing Process

# 2.1 *Two-photon absorption and materials*

The energy of a photon is given by  $h\omega$ , where h and  $\omega$  are Planck's constant divided by  $2\pi$  and the angular frequency of light, respectively. The electron is raised to an excited state when it absorbs the energy of a single photon, which is equal to  $h\omega = E_1 - E_2$ , where  $E_1$  and  $E_2$  are the energy levels ( $E_1 > E_2$ ). In the case of two-photon absorption (TPA), two photons, each with half of the energy of the gap between the two levels, induce the electron transition. So, TPA is induced only when high-power light is illuminated. (17) Ti:Sapphire lasers are widely used for inducing TPA because they produce ultrahigh-power pulses with a pulse width of approximately 100 femtoseconds (fs) or less. Furthermore, it is very useful for TPP because it has a central wavelength of approximately 800 nm, which is close to half of the wavelength of the polymerization. This enables easy control of the polymerization threshold energy. Figure 1 illustrates the sub-diffraction limit of fabrication accuracy at the focal point for single-photon absorption (SPA) and TPA. If light near to the threshold energy is used, it is possible to fabricate a sub-diffraction-limit voxel. In addition, judging from the derivative distribution, the voxel size depends more sensitively on the variation of light intensity for TPA than for SPA, implying a more pronounced threshold effect for the former possess.

TPA materials have been attracting much interest in recent years because of their wideranging applications in such areas as fluorescence imaging, optical data storage, lithographic microfabrication and photodynamic cancer therapy. The TPA material used in this work is a mixture of urethane acrylate monomers and a photoinitiator. The density of the photoinitiator is 0.1 wt%. The absorption and fluorescence wavelengths of the photoinitiator are 411 nm and 472 nm, respectively: The photoinitiator absorbs 411-nm-wavelength light and emits 472-nm-wavelength light. Radicals are activated when 472-nm-wavelength light is illuminated.

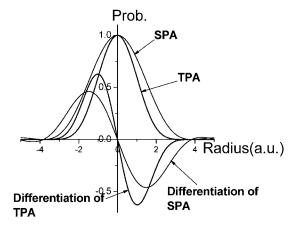


Fig. 1. Absorption probabilities and their differentiation for SPA and TPA.

#### 2.2 Minimization of voxel size

The resolution of the microstructures fabricated using the nRP process is determined by the size of a voxel (volumetric pixel). If the intensity distribution of the laser beam is assumed to be Gaussian, its geometric properties are as follows.<sup>(19)</sup>

$$\frac{r_c^2}{w_0^2} - \frac{z^2}{(b/2)^2} = 1\tag{1}$$

$$w_0 = \left(\frac{2\lambda f}{\pi d}\right) \qquad b = \frac{2\pi w_0^2}{\lambda} \tag{2}$$

Here,  $w_0$ , f, d, b, z, and  $\lambda$  are the beam waist, focal length, beam diameter, Rayleigh range, optical axis and wavelength, respectively. The intensity profile in the focal plane is

$$H(r) = H(0) \exp\left(\frac{-2r^2}{r_c^2}\right), \quad H(0) = \left(\frac{2}{\pi r_c^2}\right)P,$$
 (3)

where H(r) is the intensity of laser per unit area,  $r_c$  is the radius of a beam contour along the z-axis, and P is the laser power. The exposure energy of the laser for TPP can be expressed using eq. (4), as shown in the following, because the probability of TPP is occurring proportional to the square of the laser intensity<sup>(20)</sup>

$$E(r,z,t) \propto \left[ H(0) \exp\left(\frac{-2r^2}{r_c^2}\right) \right]^2 \cdot t \text{ or } E(r,z,t) = \alpha \left[ H(0) \exp\left(\frac{-2r^2}{r_c^2}\right) \right]^2 \cdot t,$$
 (4)

where E is the exposure energy of the laser for a time interval t and  $\alpha$  is a proportionality constant. When the exposure energy of the laser (E) is equal to the threshold exposure energy ( $E_{th}$ ) for TPA polymerization in eq. (4), the diameter of a voxel can be given as eq. (5).

$$d(P,t) = 2r_{z=0} = w_0 \left\{ \ln \left( \frac{4P^2t}{\pi^2 w_0^4 E_{th}} \right) \right\}^{\frac{1}{2}}$$
 (5)

In addition, the height, l, (r=0) of a voxel can be expressed as eq. (6).

$$l(P,t) = 2z_{r=0} = \frac{2\pi w_0^2}{\lambda} \left\{ \left( \frac{4P^2t}{\pi^2 w_0^4 E_{th}} \right)^{\frac{1}{2}} - 1 \right\}^{\frac{1}{2}}$$
 (6)

# 3. Experimental Methods

## 3.1 *nRP system and its operation*

A femtosecond laser system and the optical instruments for the nRP process are shown both in Figs. 2(a) and 2(b), which shows a photograph of the actual experimental system. A mode-locked Ti:sapphire laser was used in the system. It provided a wavelength of 780 nm and a pulse width of less than 100 fs at a repetition rate of 80 MHz. The beam was scanned on the focal plane using a two-galvano-mirror set with a resolution of approximately 2.5 nm per step, and along the vertical axis using a piezoelectric stage. The laser was tightly focused with an objective lens (NA  $1.25 \times 100$ , immersion oil used) on the photopolymerizable resin as described above which was placed on a microscopic coverglass substrate. A high-speed shutter mechanism was applied to obtain an exposure time of less than 1 ms. In the proposed mechanism, a pin-hole plate was employed to reduce the tilting angle of the galvano-mirror shutter to under one degree in the on/off control of the laser beam. The shutter, scanner, and piezoelectric stage were controlled using a computer system. The progress of the fabrication process can be monitored exactly using a high-magnification charge-coupled-device (CCD) camera, as shown in Fig. 2(a).

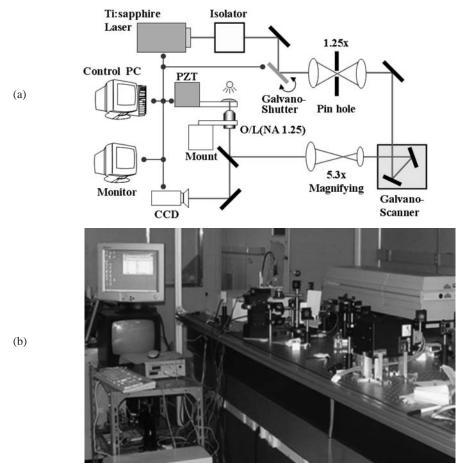


Fig. 2. (a) Schematic diagramand and (b) photograph of nanoreplication-printing (nRP) system for fabrication of nanoscale patterns and three-dimensional microstructures.

In the nRP process, a raster graphics type of voxel matrix, which was transformed from a bitmap figure file, was used to scan a pattern shape without any computer-aided-design (CAD) data. Figure 3(a) shows a voxel matrix transformed from a bitmap figure and the procedure of the voxel matrix scanning (VMS) technique. A black-and-white bitmap image is converted to a voxel matrix, which consists of '0' s for white pixels and '1' s for black pixels. In general, a large voxel matrix is required to fabricate a precise replica. The on-off control of the laser beam is determined by the elements of the voxel matrix; in case of '1' elements in the voxel matrix, the shutter is opened to generate voxels; in the other case, the shutter is closed.

The full size of a replicated figure is dependent on the distance between neighboring voxels and the voxel diameter which is determined by the laser power and the exposure time. Therefore, the desired size of pattern can be easily obtained by changing these parameters. The thickness of the glass plate shown in Fig. 3(b) needs to be very thin, less than 200  $\mu m$ , due to the very short working distance of the beam. Using the CCD monitoring device, the position of a voxel can be manipulated on the surface of the glass plate. However, much experience is required to focus a laser beam on the glass plate accurately. In the developing process, the remanent liquid-state monomer can be eliminated by dropping several ethanol droplets on the patterns.

## 3.2 Process parameters for precise patterning

The distance between neighboring voxels is one of the most important parameters for the fabrication of a precise and smooth pattern which can be obtained from the minimum distance between voxels. The minimum distance is dependent on the resolution of the galvano-mirror scanner. In this work, the step of the scanner was set to be approximately 2.5 nm in the x-axial and y-axial directions. When the minimum distance is input to fabricate a precise replica, the total size of the replica is reduced for the same voxel matrix used. To fabricate the same size of replicated pattern with the minimum distance applied, the size of the voxel matrix, which is dependent on the file size of the original bitmap figure, has to be enlarged; a more detailed bitmap figure file is required.

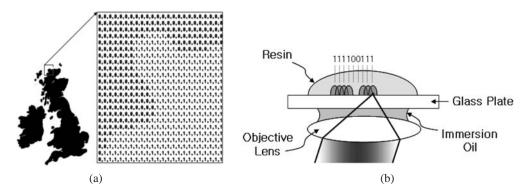


Fig. 3. (a) The bitmap file of a map of England is transformed to voxel matrix form: The rectangular box shows a partial matrix of the fully transformed voxel matrix. (b) The voxel matrix scanning (VMS) procedures; a laser beam is scanning along a row of the voxel matrix; a '1' represents the laser beam being on; a '0' the laser beam being off. The center of a voxel is located in the coordinate of each '1' of the voxel matrix.

In addition, the resolution of the fabricated pattern is related to the size of a single voxel; the lateral and axial dimensions of a voxel. Considering eqs. (5) and (6) relating to the voxel dimensions, several experiments were attempted to obtain the minimum voxel size by varying the laser power and the exposure time. From the results of the experiments in this work, the minimum lateral dimension of a voxel of approximately 200 nm was obtained, as shown in Fig. 4(a), under the conditions of 2 ms exposure time and 5 mW laser power. A comparison of the lateral dimension of voxels obtained by preliminary experiments with that of theoretical estimates is depicted in Fig. 4(b).

An important issue for obtaining a pattern by the nRP process is truncation, which happens when the laser beam is focused near the substrate surface. On the other hand, if the laser is focused far above the substrate surface, a floating pattern would be formed, which could drift away during the developing process. To solve this problem, Sun *et al.*<sup>(21)</sup> proposed an ascending scan method, in which a series of voxels were fabricated under the same irradiation conditions but their heights above the substrate were increased gradually using the ascending scan method. Figure 5 shows the truncation phenomenon and the height of a pattern fabricated using the nRP process.

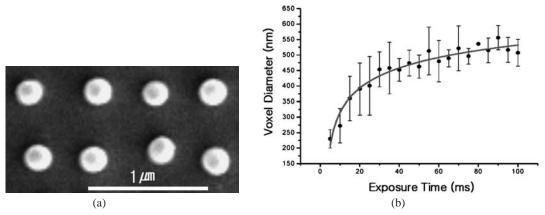


Fig. 4. (a) Minimum voxel size for laser power of 5 mW; exposure time of 2 ms. (b) Comparison between a voxel diameter of the experimental results and that of the theoretical curve (continuous curve).

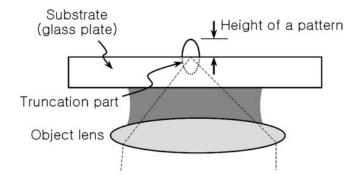


Fig. 5. Schematic diagram of focusing configurations; the polymerized part and truncated part of patterns.

## 4. Experimental Results and Discussion

## 4.1 Direct patterning using nRP process

Several patterns and figures were fabricated directly using the nRP process to demonstrate the usefulness of this work. To realize a precise patterning process, the process parameters were optimized in this work: laser power, 5 mW; exposure time, 1 ms; distance between voxels, 25 nm. A contour offset algorithm (COA) was proposed to improve the precision of the replicated patterns. In the COA, the shape-error terms that were generated in the outline of the pattern due to the lateral dimension of the voxels can be eliminated by constructing a new voxel matrix. All of the patterns in this work were fabricated by applying the COA algorithm to reduce the shape-error terms. Figures 6(a)-6(c) show the replicated figures on a scale of approximately  $10~\mu m$  or more by using the nRP process. As shown in Fig. 6, any kind of bitmap figure file that consists of a black-and-white-image, can be replicated over 10~microns with nanoscale details. Therefore, patterning using the nRP process is simple and cost-effective for fabricating a number of miniature applications.

Atomic-force microscopy (AFM) allows the evaluation of the height of a fabricated pattern and its surface roughness. In Figs. 7(a) and 7(b), the surface condition of a fabricated pattern (Fig. 6(b)) is shown, which was measured by AFM (XE-100 model,

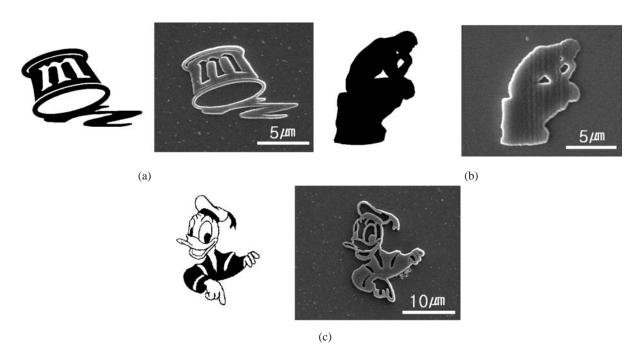


Fig. 6. SEM images of figures fabricated using nRP process; (a) the logo of center for nanoscale mechatronics & manufacturing, (b) "The Thinker," and (c) "Donald Duck."

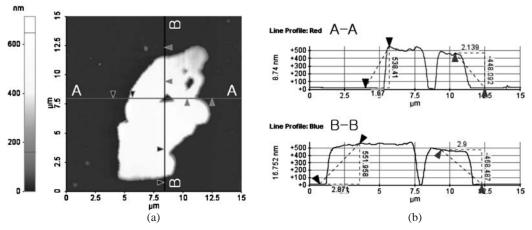


Fig. 7. AFM images of replicated two-dimensional pattern, "The Thinker"; (a) line profiles, (b) 2D analysis (AFM: XE-100 model, PSIA).

PSIA). The height of the replicated two-dimensional pattern which looks like Rodin's "The Thinker," was approximately 500 nm and the surface roughness was seemingly uniform with an *Ra*-value (average roughness) of 56.76 nm. The height of patterns can be controlled using the piezoelectric stage along the z-axis within the total length of a voxel.<sup>(21)</sup>

# 4.2 Fabrication of three-dimensional structure

The fabrication of a 3D structure was attempted using a lamination technique. The layers photopolymerized using the nRP process were stacked to fabricate a 3D structure. This technique, as one of the branches of micro-stereolithography ( $\mu$ SL), <sup>(23)</sup> is a promising technique for the fabrication of 3D structures with a resolution of the order of the optical diffraction limit. <sup>(5)</sup> A honeycomb structure was fabricated using the laser-beam scanning method layer-by-layer without the use of any sacrificial layers, which would be difficult using the general lithography technique. After accomplishing the polymerization of one layer in the process of lamination, the working plate was moved by using the piezoelectric stage 200 nm along the vertical axis of the plate to enable the fabrication of another layer. When the fabrication of the 3D laminated structure was finished, a droplet of ethanol was dropped onto the working plate as a developing process to remove the unnecessary remanent liquid resin leaving only the polymerized feature on the working plate. Figures 8(a)–8(d) show the design and the SEM images of the fabricated structure.

The shrinkage phenomenon, which can be seen in Figs. 8(c) and 8(d), occurred due to an increase in density of the liquid resin during the polymerization process, which was 11.98% in the lateral direction and 19.8% in the height direction relative to the dimensions of the bottom and top surfaces, respectively. To suppress the shrinkage phenomenon, a solgel precursor-included photopolymer was introduced in the last work. (24)

In future work, the shrinkage problem should be studied intensively to improve the precision of the fabrication of 3D microstructures for various applications. Moreover, at present, the lateral surface of the fabricated structure is too rough. Therefore, the stacking thickness has to be reduced to less than 50 nm to improve the surface condition of fabricated structures.

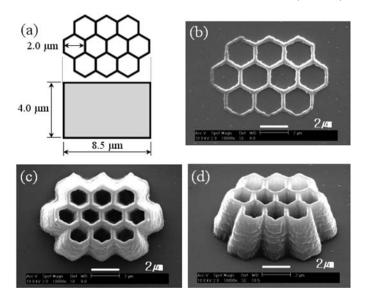


Fig. 8. 3D fabrication of honeycomb structure in resin by nRP process; (a) design and (b) SEM image of solidified bottom-layer structure, (c)–(d) SEM images of completed 3D honeycomb structure with top view and inclined view.

#### 5. Conclusions

A direct patterning method utilizing the nRP process was demonstrated in this work and several patterns were fabricated. The power and exposure time of the laser beam used are major factors in determining the resolution of fabricated patterns; the resolution obtained in this work was approximately 200 nm under the conditions of laser power, 5 mW and exposure time, 1ms. The usage of high-NA (more than 1.0) focusing optics and fs laser pulses allowed the realization of direct patterning and the fabrication of arbitrary 3D structures inside liquid photocurable polymers without the use of sacrificial layers and structures. Through this work, the shrinkage phenomenon is considered as a major factor in the fabrication of 3D structures. This finding is important to understand and further develop the fabrication technology for 3D structures.

# Acknowledgment

The research work was funded by the Center for Nanoscale Mechatronics & Manufacturing of the 21st Frontier Project supported by Korean Ministry of Science & Technology.

#### References

- 1 R. D. Piner, J. Zhu, F. Xu, S. Hong and C. A. Mirkin: Science 283 (1999) 661.
- 2 S. Y. Chou, P. R. Krauss and P. J. Renstrom: Science 272 (1996) 85.
- 3 Y. Xia, J. Tien, D. Qin and G. M. Whitesides: Langmuir 12 (1996) 4033.

- 4 T. Bailey, B. J. Choi, M. Colburn, M. Meissi, S. Shaya, J. G. Ekerdt, S. V. Sreenivasan and C. G. Willson: J. Vac. Sci. Technol. B 18 (2000) 3572.
- 5 M. D. Austin, H. Ge, W. Wu, M. Li, Z. Yu, D. Wasserman, S. A. Lyon and S. Y. Chou: Appl. Phys. Lett. 84 (2004) 5299.
- 6 S. Maruo and S. Kawata: J. Microelectromechanical Systems 7 (1998) 411.
- 7 H. -B. Sun, K. Takada and S. Kawata: Appl. Phys. Lett. **79** (2001) 3173.
- 8 P. Galajda and P. Ormos: Appl. Phys. Lett. 78 (2001) 249.
- 9 S. Kawata, H.-B. Sun, T. Tanaka and K. Takada: Nature **412** (2001) 697.
- 10 J. Serbin, A. Egbert, A. Ostendorf, B. N. Chichkov, R. Houbertz, G. Domann, J. Schulz, C. Cronauer, L. Frohlich and M. Popall: Opt. Lett. 28 (2003) 301.
- 11 H. -B. Sun, S. Matsuo and H. Misawa: Appl. Phys. Lett. **74** (1999) 786.
- 12 H.-B. Sun, M. Maeda, K. Takada, J. W. M. Chon and M. Gu, S. Kawata: Appl. Phys. Lett. 83 (2003) 819.
- H. -B. Sun, Y. Xu, S. Juodkazism K. Sun, M. Watanabe, S. Matsuo, H. Misawa and J. Nishii: Opt. Lett. 26 (2001) 325.
- 14 K. Kaneko, H.B. Sun, X.M. Duan, S. Kawata: Appl. Phys. Lett. 83 (2003) 2091.
- 15 T. Tanaka, H.-B. Sun and S. Kawata: Appl. Phys. Lett. 80 (2002) 312.
- 16 E. -Y. Pan, N. -W. Pu, Y. -P. Tong and H. -F. Yau: Appl. Phys. B 77 (2003) 485.
- 17 Y. R. Shen: The Principles of Nonlinear Optics (John Wiley & Sons, Singapore, 1984) p. 202.
- 18 S. W. Yi, S. K. Lee, H. J. Kong, D. -Y. Yang, S. H. Park, T. W. Lim, R. H. Kim and K-. S. Lee: Proc. of SPIE. **5342** (2004) 137.
- 19 A. L. Schawlow, A. E. Siegman, T. Tamir: Springer Series in Optical Science Volume 1 (Springer, 1999) p. 200.
- 20 W. Denk, J. H. Strickler and W. W. Webb: Science 248 (1990) 73.
- 21 H.-B. Sun, T. Tanaka and S. Kawata: Appl. Phys. Letter. 80 (2002) 3673.
- 22 T. W. Lim, S. H. Park, D. -Y. Yang and H. J. Kong: J. of Korean Society of Precision Engineering 21 (2004) 160.
- 23 X. Zhang, X. N. Jiang and C. Sun: Sensors and Actuators 73 (1999) 149.
- 24 H. K. Yang, M. S. Kim, S. W. Kang, K. S. Kim, K. S. Lee, S. H. Park, D. -Y. Yang, H. J. Kong, H. -B. Sun, S. Kawata and P. Fleitz: J. Photopolym. Sci. Technol. 17 (2004) 385.